High-Throughput Small Molecule Identification Using MALDI-TOF and a Nanolayered Substrate

ARTICLE *in* ANALYTICAL CHEMISTRY · JUNE 2011

Impact Factor: 5.64 · DOI: 10.1021/ac2006735 · Source: PubMed

6 AUTHORS, INCLUDING:

Hak Soo Choi
Beth Israel Deaconess Medical Center
95 PUBLICATIONS **4,344** CITATIONS
SEE PROFILE

Khaled A Nasr
University of Texas Southwestern Medical C…
23 PUBLICATIONS **557** CITATIONS
SEE PROFILE

analytical chemistry

ARTICLE

pubs.acs.org/ac

High-Throughput Small Molecule Identification Using MALDI-TOF and a Nanolayered Substrate

Jeong Heon Lee,[†,‡] Hak Soo Choi,[†,‡] Khaled A. Nasr,[†,‡] Miyoung Ha,[§] Yangsun Kim,[§] and John V. Frangioni*[,†,‡,∥]

[†]Robotic Chemistry Group, Center for Molecular Imaging, Beth Israel Deaconess Medical Center, Boston, Massachusetts 02215, United States

[‡]Division of Hematology/Oncology, Department of Medicine, Beth Israel Deaconess Medical Center, Boston, Massachusetts 02215, United States

[§]Hudson Surface Technology, Fort Lee, New Jersey 07024, United States

[∥]Department of Radiology, Beth Israel Deaconess Medical Center, Boston, Massachusetts 02215, United States

Supporting Information

ABSTRACT: Encoderless combinatorial chemistry requires high-throughput product identification without the use of chemical or other tags. We developed a novel nanolayered substrate plate and combined it with a microarraying robot, matrix-assisted laser desorption/ionization (MALDI) mass spectrometry, and custom software to produce a high-throughput small molecule identification system. To optimize system performance, we spotted 5 different chemical entities, spanning a m/z range of 195 to 1338, in 20,304 spots for a total of 101,520 molecules. The initial spot identification rate was 99.85% (20,273 spots), and after a proofreading algorithm was added, 100% of 20,304 spots and 101,520 molecules were identified. An internal recalibration algorithm also significantly improved mass accuracy to as low as 45 ppm. Using this optimized system, 47 different chemical entities, spanning a m/z range of 138 to 1,592, were spotted over 5,076 spots and could be identified with 100% accuracy. Our study lays the foundation for improved encoderless combinatorial chemistry.

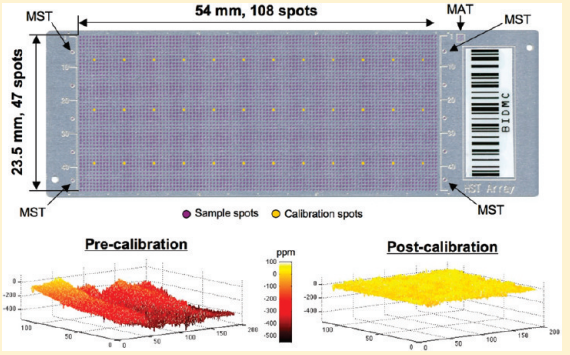

Nanoscale materials and technology have led to many recent developments in molecular imaging, diagnostics, and drug discovery.[1−5] However, development of ideal ligand molecules for use as diagnostic, therapeutic, and theragnostic agents is still time-consuming and costly.[4,6]

Small molecules have been considered for use as potential targeting ligands, and much effort has been directed toward the development of molecules that are disease-specific.[7−10] Potential drug candidates are often generated by combinatorial chemistry, screened using high-throughput assays, and identified by high-throughput analysis.[11−13] Unfortunately, analytical aspects of this process have lagged. Chemical spaces created by combinatorial libraries are increasingly larger and faster than target identification technologies.[14,15] Therefore, there is an imperative to develop high-speed, highly accurate identification systems as more synthetic molecules are created by combinatorial techniques.

Schreiber et al. reported using chemical encoding of each library building block, but the chemical steps are rather complicated.[12] Matrix-assisted laser desorption/ionization (MALDI) time-of-flight (TOF) is one possible system to elucidate unknown chemicals, without use of an encoding process (i.e., encoderless detection), due to its direct and single-step analysis.[16−18] Instrument features, such as laser repetition rate and high-speed movement of the laser between spots, are potential advantages that can only be realized if offline sample preparation is performed efficiently. Recently, Woodbury et al. developed a MALDI-MS based approach to identify the chemical composition of an *in situ*-synthesized microarray directly on the array features.[19] Unfortunately, this approach is not useful for an individual spot of molecules generated from a typical combinatorial synthesis. A more general and versatile MALDI identification system would provide postsynthesis sample imprinting in a high-density array format, although neither the technology nor the methodology for such a format has been described to date. In this study, we hypothesized that a precise, nanolayered substrate could provide the basis for a novel technology capable of fully automated, high-throughput identification of small molecules at the nanoliter scale.

EXPERIMENTAL SECTION

Chemicals. All chemicals and solvents were American Chemical Society grade or higher. MALDI matrixes, 9-aminoacridine

Received: March 16, 2011
Accepted: May 23, 2011
Published: June 08, 2011

(9-AA), meso-tetrakis(pentafluorophenyl)porphyrin (F20TPP), and 2,5-dihydrobenzoic acid (DHB) were purchased from either Sigma-Aldrich (St. Louis, MO) or Bruker Daltonics (Billerica, MA). For preparing standard samples, RGD (Arg-Gly-Asp) and cRGDyk (cyclo Arg-Gly-Asp-D-Tyr-Lys) were purchased from AnaSpec (Fremont, CA). PG35C and GS-PEP were synthesized as previously described.[20,21] All other chemicals were commercially available unless noted otherwise. Log D at pH 7.4 and pK_A (the most ionic form) were calculated using the Marvin Calculator Plugin of JChem (ChemAxon, Budapest, Hungary).

High-Density Micropatterned Array (HDMA) Plate. A nanolayered, metal-based array plate (HDMA; 75 mm × 25 mm × 0.3 mm size) was developed with the assistance of Hudson Surface Technology, Inc. (HST; Newark, NJ) and was adapted to our MALDI-TOF and MALDI imaging system. In summary, the HDMA plate was prepared by (a) chemical etching of the substrate exposed by the first photoresist patterning, (b) forming array guides with physical teaching points on the substrate by removing the first pattern, (c) forming a second photoresist pattern as a spot array inside the guides, (d) forming a silane-based hydrophobic nanolayer on the substrate, and (e) removing the second photoresist pattern to form an uncoated spot array portion from the hydrophobic nanolayer (Figure S-1 in the Supporting Information). The silanol nanolayer was characterized using ellipsometry and scanning electron microscopy. Spatial spacing in the array is 500 μm and each grid has a hydrophilic circle with a 300 μm diameter. A total of 5 040 sample spots and 36 calibration spots were spotted on each HDMA plate. Additionally, four spots were generated on the top-right side for microarray teaching and one on each corner of the array for MALDI-MS teaching. A special magnetic plate holder, which included three point magnets per HDMA plate, was designed to mount four HDMA plates at the same time.

Instrumentation. DHB in dimethylsulfoxide (DMSO) was prespotted onto the HDMA plate using a prototype of a piezoelectric inkjet printer (μMatrix Spotter, HST). Small molecules were prepared as 1−5 mM stock solutions in DMSO and 10 μL of each sample was distributed in a polypropylene 384-well plate. A contact type microarraying robot (OmniGrid Accent, DigiLab, Inc., Holliston, MA) mounted with SMP11 pins (ArrayIt, Telechem, Sunnyvale, CA) were used to spot the compounds over the DHB preloaded HDMA plate. The HDMA plate micropatterning was designed to correspond exactly with the pin geometry of the microarraying robot. Matrix crystal images were obtained using a Nikon Eclipse TE-300 epifluorescence microscope equipped with a 100 W mercury light source. Standard filter sets (Nikon) were comprised of the following excitation/dichroic/emission filter wavelengths: blue (340−360 nm/400 nm/430−490 nm), green (460−500 nm/505 nm/505−560 nm), and red (525−555 nm/565 nm/590−650 nm), respectively. All mass spectra were collected using the UltraFlex III MALDI TOF/TOF system (Bruker Daltonics, Billerica, MA) equipped with a SmartBeam laser operating at 100 Hz and set to an extraction voltage of 25 kV in reflectron mode. Custom scripts for AutoXecute (Bruker Daltonics) were used for automated mass acquisition. Spectra were processed using the Compass 1.2 SR1 package (Bruker Daltonics) with added custom FlexAnalysis (Bruker Daltonics) scripts and custom Excel 2007 macros. Postprocessing for mass calibration was carried out using the 36 calibration spots, each containing 5 mass standards spanning the m/z range of 195 to 1 338, on each HDMA plate. Data plotting and visualization were performed by MATLAB (MathWorks, Inc., Natick, MA) and FlexImaging software (Bruker Daltonics).

RESULTS AND DISCUSSION

Engineering of the HDMA Plate. The 75 mm × 25 mm HDMA plate was engineered for compatibility with a standard glass slide typically used for microarraying (Figure 1A). The plate was also designed to have highly precise, micropatterned, hydrophobic spot arrays generated by photolithography after coating the stainless steel surface with a hydrophobic nanolayer (Figure 1B and Figure S-1 in the Supporting Information). The process of surface patterning was modified from a previously described photoresist patterning method.[22] After the first photolithography, the chemical etching process formed array guides, which included both microarrayer teaching spots (MAT) and MALDI-TOF teaching spots (MST). The second photolithography, followed by silane coating, exposed each individual spot as a hydrophobic barrier for sample application. This is a simplified and space-efficient method compared to previous patterning, which would be further processed to generate an etched mark of the sampling area. A large-scale integration of sample spots could then be achieved to produce a high-density, array format MALDI plate that interfaced with our microarraying robot.

A total of 5 076 spots (108 rows and 47 columns), which were precisely aligned by 300 μm spots with 200 μm spatial spacing, were produced on the HDMA plate. In nanoscale sample preparation, it is essential to keep the sample solution (i.e., an organic solvent with low dielectric constant) contained on each spot without cross-contamination. The hydrophobic layer was used for sample focusing to prevent the solvent from striking out and producing a concentrated, homogeneous matrix-analyte crystal. Magnets were used to tightly restrain each HDMA plate onto the plate holder and to ensure flatness, as each plate is only 0.3 mm thick (Figure 1C). From this setup, a total of 20 304 chemical spots could be produced on four HDMA plates (i.e., 5 076 spots per plate).

Optimization of Sample Preparation. In order to successfully spot samples on the plate at the nanoscale, an optimal solvent system, which is compatible with both the microarrayer and MALDI-MS systems, had to be chosen.[23,24] DMSO is used to dissolve a wide range of polar and nonpolar organic molecules due to its dynamic viscosity (1.996 cP at 20 °C), high dielectric constant (47.2), and high boiling temperature (189 °C). Therefore, DMSO permits easy transfer of samples from the 384-well plate to the HDMA plate and evaporates within 10 min due to the nanoliter loading volume of the samples.

MALDI matrix solution was prespotted onto the HDMA plate using a piezoelectric inkjet printer, which had an inherent resolution of 5 760 × 1 440 dpi. The matrix solution was dispensed in multiple 3 pL bursts to achieve a 300 μm final diameter of matrix at each of the 5 076 spot positions. The total matrix printing time was ≈30 s per HDMA plate. Figure 2 shows different crystallization patterns of DHB in DMSO (left) or 70% methanol (right) as a function of solvent volume and dispensing condition. The spots were coated onto an indium−tin-oxide (ITO)-coated microscope slide (HST, Inc.), which has high UV transparency and surface hydrophobicity. Spots were imaged on a UV-compatible fluorescence microscope.

DHB crystals were first prepared by a typical dried droplet method with large volume (0.5 μL) in order to verify the effect of solvent (Figure 2A). The DMSO solution was dried in a vacuum oven (equipped with a pump pressure of 6.7 × 10^2 Pa) at 45 °C for 10−12 min. Although DMSO has a higher boiling point and slower evaporation rate than conventional matrix solvents (i.e.,

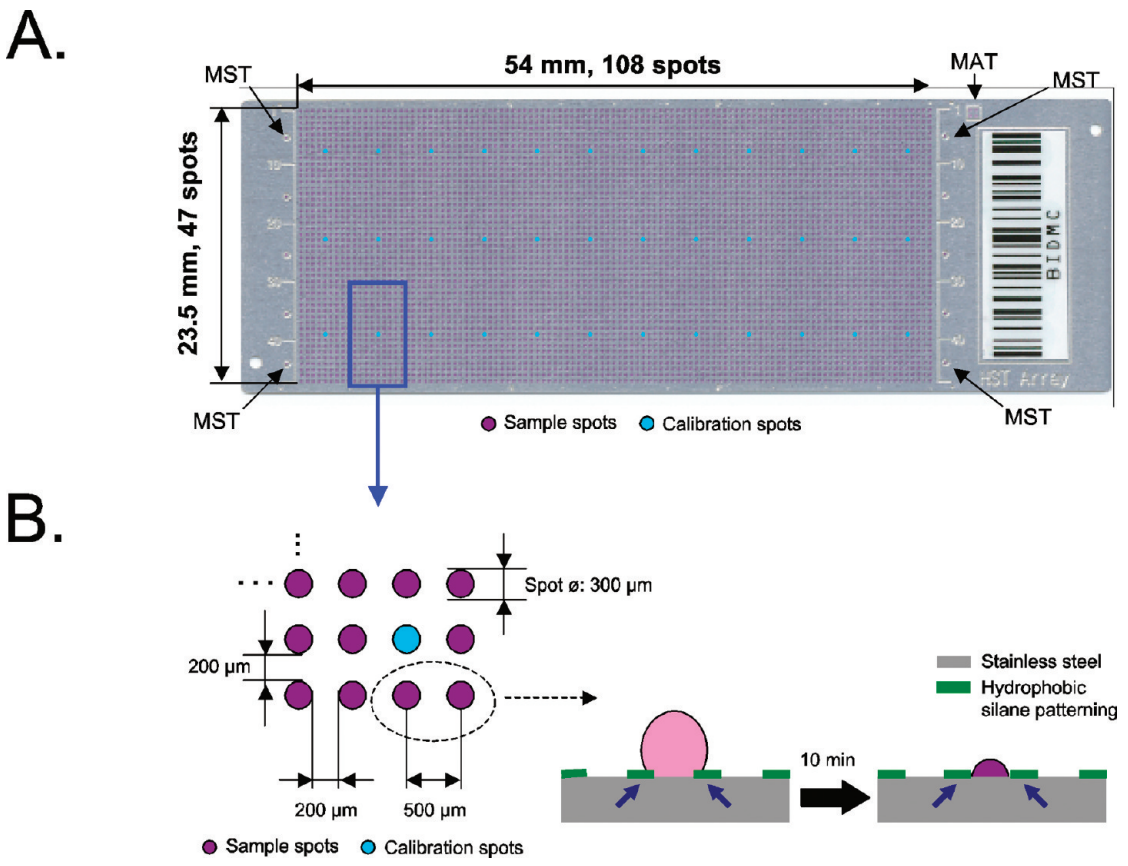

Figure 1. High-density micropatterned array (HDMA) plate: (A) an actual HDMA plate with 5 040 sample spots (purple) and 36 calibration spots (yellow). MAT = Microarrayer teaching spots (4 total). MST = MALDI-TOF teaching spot (1 in each of 4 positions). (B) A schematic of micropatterned spots (left) after sample focusing by hydrophobic nanolayer constraint (right). (C) Schematic (left) and actual HDMA plate holder (right).

70% methanol in water), DHB in DMSO eliminated formation of matrix complexes and resulted in improved crystal homogeneity, which eventually increased the detection yield significantly.[25] DHB provides multiple donor sites for hydrogen-bonding (i.e., 2,5-dihydroxyl group); therefore, the solvation effect of DHB in DMSO results in homogeneous and well-distributed crystal formation because DMSO does not form a hydrogen-bonding network by itself.[26] In addition, intermolecular dipole interactions of DHB molecules to form crystal structures can be disrupted by strong hydrogen bonding acceptor sites (S═O group).[27−29] This pattern was also seen with nanoliter volumes (dispensed by a microarraying robot, Figure 2B), but small crystals were formed. The solvent effect was minimized during repetitive inkjet dispensing (Figure 2C) due to picoliter dispensing volumes and ultrafast drying time.[30] Crystals were larger (≈50 μm), although confined to the desired circular spot area, and still produced excellent MALDI sensitivity. Optimal parameters for inkjet dispensing included a DHB stock solution of 80 mg/mL in DMSO, which resulted in 100 ng of DHB per spot (Table S-1 in the Supporting Information).

Automated, high-throughput sample deposition onto HDMA plates was performed using a nanoliter microarraying robot (OmniGrid Accent, DigiLab). The advantages of such a strategy include high-speed liquid delivery with nanoliter sample volume and precisely aligned and reproducible spots.[31] Chemicals created from combinatorial chemistry are commonly prepared in a 384-well plate format by a liquid handler.[13] Robotic imprinting compressed chemical information from the area of a single well of 384-well plate to a 300 μm diameter spot (a 192-fold compression). After 25 blotting spots, microarray pins (SMP11, ArrayIt) delivered approximately 3 nL of sample in DMSO to create a 300 μm diameter spot with a 25 ms contact time. The mass of sample yielding the highest MALDI signal was 6.6 ng per spot (Table S-1 in the Supporting Information). Nanoliter sample spotting leads to better signal intensity and sensitivity than microliter dispensing with the same quantity of analytes.[32] To validate homogeneous incorporation of analytes into the matrix crystal, we selected Alexa Fluor 555 (Alexa555; Invitrogen) as a model compound. Alexa555 in DMSO (1 mM) was printed on the DHB prespotted ITO slide, while the same amount of Alexa555/DHB mixture was printed directly on the plain ITO slide. As shown in Figure S-2 in the Supporting Information, the fluorescence signal from Alexa555 (600 nm) completely overlapped the signal from the DHB crystals (400 nm), with no significant difference seen between the prespotted DHB (Figure S-2A in the Supporting Information) and the mixture of DHB (Figure S-2B in the Supporting Information). In addition, both crystals showed identically strong MS signals from the Alexa555 compound (Figure S-2 in the Supporting Information).

Optimization of Automated MS Acquisition. To establish a reference for instrument optimization, five different molecules were selected as standard compounds: 9-AA (m/z 195.09), RGD (m/z 347.12), cRGDyK (m/z 620.32), PG35C (m/z 1003.41), and GS-PEP (m/z 1338.71), a mixture of which was prepared

dx.doi.org/10.1021/ac2006735 |*Anal. Chem.* 2011, 83, 5283–5289

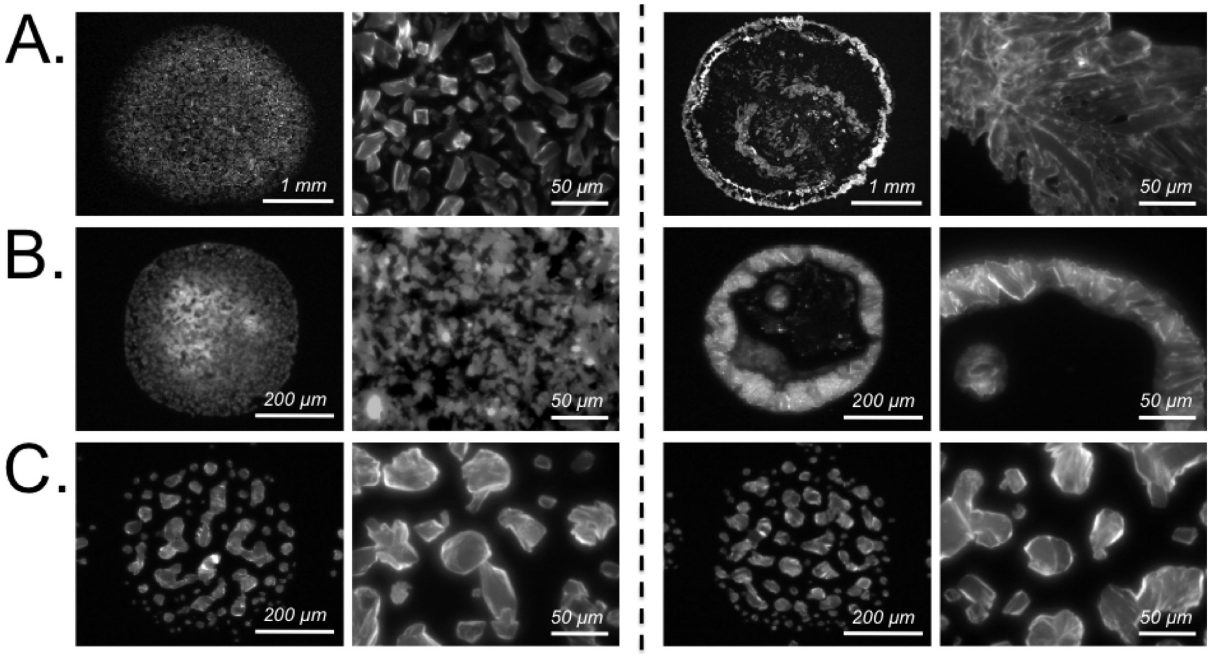

Figure 2. Crystallization patterns of DHB in DMSO (left) and 70% methanol in water (right): DHB stock solutions were loaded onto an ITO slide by a pipet (A), the microarrayer (B), and the piezoelectric inkjet printer (C) and viewed using UV fluorescence.

in DMSO. A molar ratio of each compound was adjusted to display approximately equal ionization yield (Figure 3A). In the following step, as described in Table S-1 in the Supporting Information, the matrix-to-analyte ratio was optimized by spotting approximately 6.6 ng (molar amount of each sample was defined as 0.9 pmol of 9-AA, 4.5 pmol of RGD, 1.7 pmol of cRGDyK, 3.4 pmol of PG35C, and 0.5 pmol of GS-PEP) of standard samples onto the DHB (100 ng) preloaded spot. The standard samples were spotted onto HDMA plates by microarraying, and a total of 20 304 identical spots comprising 101 520 compounds were prepared within 150 min.

The integrated, high-throughput system we developed for small molecule identification included a MALDI-MS system and several custom analysis scripts (Figure S-3 in the Supporting Information). As described above, the standard samples could be prepared on the HDMA plate by the microarraying robot and transferred to the MALDI-MS spectrometer without having to change the instrument geometry. A geometry file for four HDMA plates was exported from FlexImaging software, and an AutoXecute sequence was programmed for continuous MS scanning. Instrument parameters for single spot detection were optimized and found to be 50 μm for the laser focus, 300 laser shots, and 50 μm rastering in 6 different positions (Table 1).

In high-throughput and automated MALDI systems, it is often difficult to achieve high sensitivity from a single sample spot without affecting nearby sample spots. On one hand, increasing laser irradiation strongly increases ion production.[33] On the other hand, if laser irradiation is too high, then adjacent spots could be sampled or destroyed. Through preliminary experiments, we determined that adjustment of the laser to 60% of maximum and a 100 Hz repetition rate provided excellent surface desorption without affecting nearby spots. We also ensured that laser irradiation (50 μm in diameter) started from the center portion of the 300 μm diameter spot and continued in the center-right direction such that $\leq$25% of the entire spot area was irradiated. MALDI stage movement was also optimized for maximum speed and accuracy.

Data acquisition from the 20 304 spots on the 4 HDMA plates took 40 h and produced a 22 GB data set. Once initial MS scanning was completed, the raw data set was processed, which included proofreading and internal recalibration. Several custom scripts in the FlexAnalysis and Excel 2007 macros were developed and linked as semiautomatic sequences. From the initial MS scanning of the 20 304 spots containing 5 different molecules per spot, we found 31 missing spots (99.85% spot detection rate). Although our sample preparation method dramatically increased spot uniformity and MALDI detectability, the distribution coefficient (log D, pH 7.4) and solution charge states in the matrix−analyte complex may cause some molecules to be located slightly away from the initial spot.[34] For example, the log D, pH 7.4 of 9-AA and GS-PEP, 1.19 and −10.23, respectively, vary over a wide range. By adding an automated rescanning algorithm, which increased the number of laser shots from 300 to 600 (spot coverage was increased 50% to 75%) using a custom AutoXecute XML sequence, we achieved 100% MS detection of spots and retrieved mass values that were used to create a mass table. In this proof-of-principle experiment, all 101 520 molecules could be identified based on the expected mass. The mass table could also, for example, be applied to tolerance filtering software to match and identify the final products from virtual chemical libraries (Figure S-3 in the Supporting Information).

A major challenge for acquiring accurate mass values centers around mass calibration at various physical points on the HDMA plate, which is essential for converting the TOF into m/z values.[35] In order to maximize the accuracy of the TOF constant, we divided the array on the HDMA plate into 36 groups (12 rows $\times$ 3 columns; see red square in Figure 1A), placing one calibrant spot in the middle of each square. Each calibrant spot was used to calculate the calibration constant of the spectra acquired from the rest of the spots in its group. We used 36 calibration points per

dx.doi.org/10.1021/ac2006735 |*Anal. Chem.* 2011, 83, 5283–5289

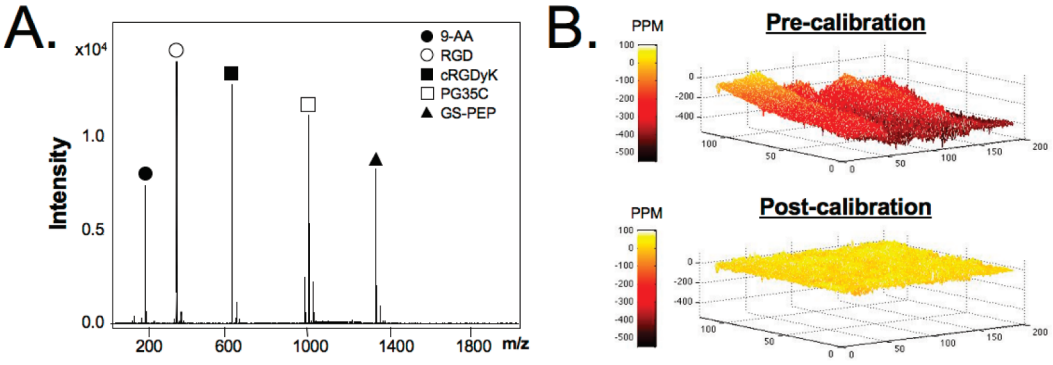

C.

Compound	[M+H]⁺	Replication	Detectability (%)	Error Pre-Calibration (ppm)	Error Post-Calibration (ppm)	Improvement (%) Pre-/Post-Calibration
9-AA	195.092	20,304	100	632	148	76.6
RGD	347.168	20,304	100	420	78	81.4
cRGDyK	620.316	20,304	100	269	54	79.9
PG35C	1,003.409	20,304	100	294	47	84.0
GS-PEP	1,338.702	20,304	100	265	45	83.0
Total		101,520	100			

Figure 3. Automated MS acquisition for 101 520 compounds on four HDMA plates: (A) MALDI spectrum of the five standard compounds covering the m/z range 195−1338. (B) Mass deviation of cRGDyK (m/z 620.316) by parts per million error before internal calibration (top) and after calibration (bottom). (C) A summary of detectability and calibration correction for each compound.

Table 1. Optimization of Physicochemical Parameters for High-Throughput MS Scanning of Nanolayered Plate

component	parameter	optimization	description				
plate	density of spot	HDMA plate	5 076 spots of 300 μm in diameter per slide with 500 μm interspot spacing				
pattern	cross-contamination of spots	hydrophobic nanolayer	prevention of cross-contamination among spots				
holder	physical flatness of plate	magnetic holder	3 magnet constraints per HDMA plate				
matrix	background signal	inkjet dispensing	homogeneity and confinement of matrix deposition; facilitates application of different matrixes				
solvent	spot uniformity	DMSO	fine crystallization and homogeneous sample distribution				
spotting	regularity of sample loading	microarrayer	pin print using nanoliter sample volume				
calibration	mass accuracy	36 calibration points	each internal calibration spot applied to 3.5 mm × 2 mm area (140 other spots)				
mass spectrometer	mechanical speed	instrument parameters	laser shots per spot	detection position per spot	rastering	detection time per spot	scanning time per 5 076 spots
			300	6	50 μm	7 s	9 h 52 min

plate, 0.71% out of the total number of spots, and applied the calibration constant to the spectra of each group using a custom FlexAnalysis script. Mass deviation of cRGDyk (m/z 620.32), for example, from 20 304 spots after MS scanning pre- (top) and postcalibration (bottom) is shown in Figure 3B. The determined m/z values after calibration had an error range of less than 54 ppm, which represented an 80% improvement (Figure 3C). The four other compounds also showed ≈80% improvement, with error ranges as low as 45 ppm, suggesting that calibration improved accuracy independent of m/z.

Identification of Small Molecules within a Library. A long-range goal of our group is to develop combinatorial, target-specific, small molecule libraries with each molecule containing a single nucleophilic amine. The primary amine is used for conjugating targeting ligands to effector molecules[36] as well as for tethering during initial target screening. A final feature of this amine is that it helps small molecules fly in the positive mode of the MS.[37] We prepared 47 primary amine-containing model compounds (Figure S-4 and Table S-2 in the Supporting Information) by dissolving in DMSO at 1−5 mM concentrations. This small molecule library represents a wide range of mass (m/z 138−1 592), log D at pH 7.4 (−12.7 to 3.1), and pK_A (2.9−12.2). Each compound was replicated 108 times on a DHB preloaded HDMA plate (i.e., 47 rows of 108 identical columns). During initial scanning, a single spot was missed, which was automatically rescanned and found. After rescanning, 100% of the 5 076 expected molecules could be identified by MS, with the results displayable as a visual representation (Figure 4).

dx.doi.org/10.1021/ac2006735 |*Anal. Chem.* 2011, 83, 5283–5289

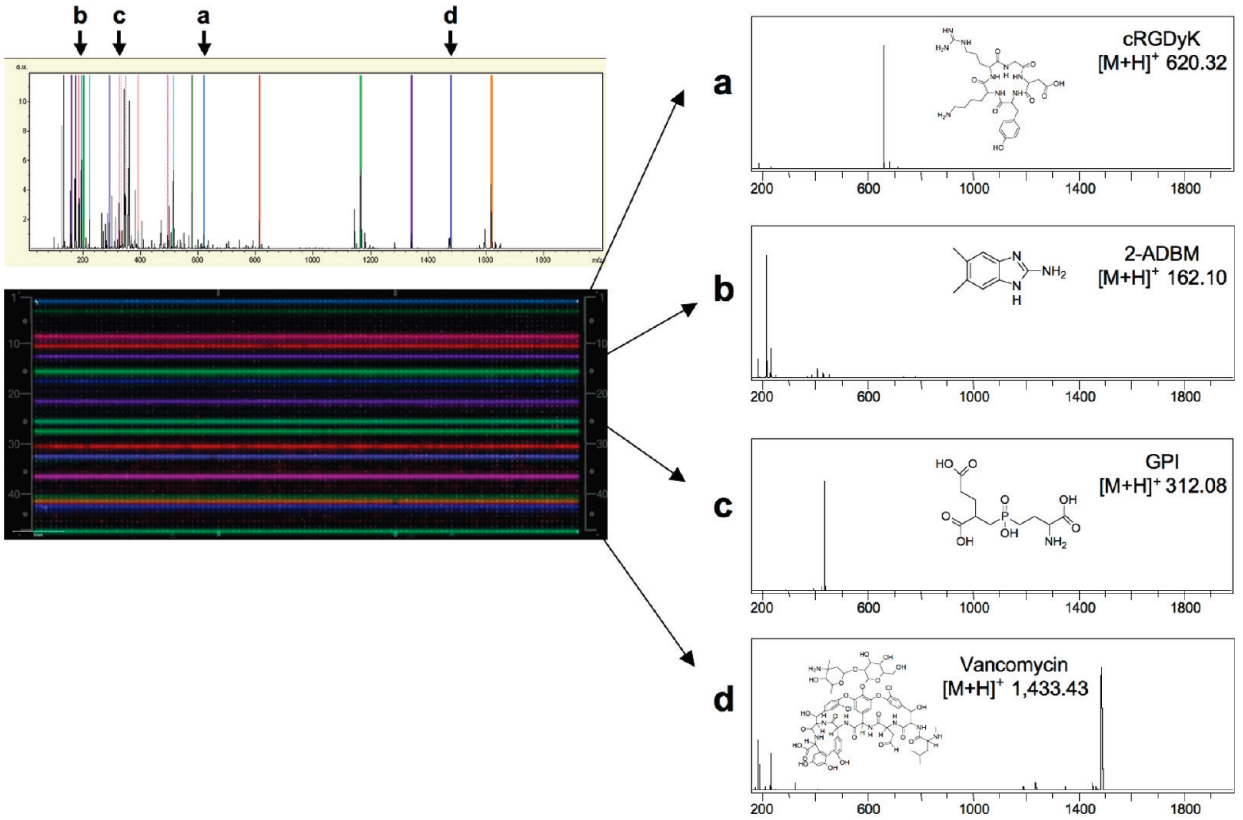

Figure 4. MALDI MS imaging for spot annotation using the HDMA geometry: A combined spectrum of 5 076 spots (top) and its color-coding examples are presented (bottom). Each color corresponds to a different mass, as shown for four example molecules **a**−**d** (right).

The complexity of small molecule library analysis by MALDI-MS is caused primarily by chemical noise, i.e., matrix signal interference.[38] When designing our system, we were careful to ensure flexibility in choosing MS matrixes. As shown in Figure S-5 in the Supporting Information, the matrix choice has a profound impact on the signal-to-background ratio for certain molecules. Because the MS instrument will hold 4 HDMA plates at a time, one could choose to scan 5 076 unknown spots with 4 different matrixes, 2 different matrixes in 2 different ion modes, or whatever is required for complete identification of unknown samples. Of course, the matrix-to-analyte ratio will likely have to be adjusted for specific applications.

MALDI detection of small molecules within a chemical library can be facilitated by certain intrinsic characteristics, which determine the initial charge state in the liquid phase, analyte incorporation in the host matrix, laser energy adsorption (i.e., primary ionization of matrix), and ion−molecule reaction in the gas phase (i.e., secondary ionization).[34,39] The primary amine group present in all of our small molecules serves to increase ionization efficiency. In an aprotic solvent, an acid−base pair could be formed by hydrogen bonding, called homoconjugation, which enhances the acidity of acids and promotes proton donation to matrix molecules.[40] When the laser irradiates a spot, positively charged analyte ions can be formed by a proton transfer reaction or cationization in the presence of salts. Indeed, all of our model small molecules produced $[M + H]^+$ or $[M + X]^+$ ions under the conditions used, although ionization efficiency of each molecule differed (signal-to-noise ratio ranged from 140 to 8 902, Table S-2 in the Supporting Information). In addition, reproducible ionization yield of the replicated molecules was confirmed by inspecting peak intensity profiles corresponding to marked color intensity (Figure 4). This same strategy could be employed for small molecule libraries with different intrinsic features, provided that all matrix and MALDI parameters were optimized accordingly.

CONCLUSIONS

By developing a nanolayered, micropatterned HDMA plate that confines nanoliter sample volume to regularly spaced spots, we were able to create an integrated, high-throughput MS detection system that is capable of analyzing up to 20 304 samples under full automation. This study lays the foundation for improved encoderless combinatorial chemistry and the development of novel diagnostic, therapeutic, and theragnostic small molecules.

ASSOCIATED CONTENT

Supporting Information. Additional information as noted in text. This material is available free of charge via the Internet at http://pubs.acs.org.

AUTHOR INFORMATION

Corresponding Author

*Address: John V. Frangioni, M.D., Ph.D. BIDMC, Room SL-B05 330 Brookline Avenue Boston, MA 02215. Office phone: 617-667-0692. Fax: 617-667-0981. E-mail: jfrangio@bidmc.harvard.edu.

■ ACKNOWLEDGMENT

We thank Brian Stall (Bruker Daltonics, Billerica, MA), Alex Allardyce (ChemAxon, Budapest, Hungary), Colin Johnson (LAE Technologies, Barrie, Canada), and Marsha Paul (Caliper Life Science, Hopkinton, MA) for technical support and many helpful discussions. We also thank Rafiou Oketokoun, Jong Seo Yoon, Conor Cross, and Tejas Gajera for assistance with development of the Robotic Chemistry System. We thank Lindsey Gendall and Lorissa A. Moffitt for editing and Linda Keys and Eugenia Trabucchi for administrative assistance. This study was supported by the following grants from the Nehemias Gorin Foundation and the National Institutes of Health: NCI BRP Grant No. R01-CA-115296 (J.V.F.), NIBIB Grant No. R01-EB-010022 (J.V.F. and H.S.C.), NIBIB Grant No. R01-EB-011523 (H.S.C. and J.V.F.), and NCI Grant No. F32-CA-132332 (K.A.N.).

■ REFERENCES

(1) Whitesides, G. M. *Nat. Biotechnol.* **2003**, *21*, 1161–1165.
(2) Frangioni, J. V. *Curr. Opin. Chem. Biol.* **2003**, *7*, 626–634.
(3) Duncan, R. *Nat. Rev. Cancer* **2006**, *6*, 688–701.
(4) Frangioni, J. V. *J. Clin. Oncol.* **2008**, *26*, 4012–4021.
(5) Wan, A. C.; Ying, J. Y. *Adv. Drug Delivery Rev.* **2010**, *62*, 731–740.
(6) Choi, H. S.; Frangioni, J. V. *Mol. Imaging* **2010**, *9*, 291–310.
(7) Houghten, R. A.; Pinilla, C.; Blondelle, S. E.; Appel, J. R.; Dooley, C. T.; Cuervo, J. H. *Nature* **1991**, *354*, 84–86.
(8) Patel, D. V.; Godon, E. M. *Drug Discovery Today* **1996**, *1*, 134–144.
(9) Geysen, H. M.; Schoenen, F.; Wagner, D.; Wagner, R. *Nat. Rev. Drug Discovery* **2003**, *2*, 222–230.
(10) Schreiber, S. L. *Science* **2000**, *287*, 1964–1969.
(11) Lam, K. S.; Salmon, S. E.; Hersh, E. M.; Hruby, V. J.; Kazmierski, W. M.; Knapp, R. J. *Nature* **1991**, *354*, 82–84.
(12) Blackwell, H. E.; Perez, L.; Stavenger, R. A.; Tallarico, J. A.; Cope Eatough, E.; Foley, M. A.; Schreiber, S. L. *Chem. Biol.* **2001**, *8*, 1167–1182.
(13) Clemons, P. A.; Koehler, A. N.; Wagner, B. K.; Sprigings, T. G.; Spring, D. R.; King, R. W.; Schreiber, S. L.; Foley, M. A. *Chem. Biol.* **2001**, *8*, 1183–1195.
(14) Lee, M. Y.; Dordick, J. S. *Curr. Opin. Biotechnol.* **2006**, *17*, 619–627.
(15) Woods, D. J.; Williams, T. M. *Invert. Neurosci.* **2007**, *7*, 245–250.
(16) Amadei, G. A.; Cho, C. F.; Lewis, J. D.; Luyt, L. G. *J. Mass Spectrom.* **2010**, *45*, 241–251.
(17) Cohen, L. H.; Gusev, A. I. *Anal. Bioanal. Chem.* **2002**, *373*, 571–586.
(18) Shroff, R.; Rulisek, L.; Doubsky, J.; Svatos, A. *Proc. Natl. Acad. Sci. U.S.A.* **2009**, *106*, 10092–10096.
(19) Greving, M. P.; Kumar, P.; Zhao, Z. G.; Woodbury, N. W. *Langmuir* **2010**, *26*, 1456–1459.
(20) Galande, A. K.; Weissleder, R.; Tung, C. H. *J. Comb. Chem.* **2005**, *7*, 174–177.
(21) Kalamajski, S.; Aspberg, A.; Oldberg, A. *J. Biol. Chem* . **2007**, *282*, 16062–16067.
(22) Kim, Y. S. *Sample plate for MALDI mass spectrometry and process for manufacture of the same*. U.S. Patent 7,619,215, November 17, 2009.
(23) Bornsen, K. O. *Methods Mol. Biol.* **2000**, *146*, 387–404.
(24) Bornsen, K. O.; Gass, M. A.; Bruin, G. J.; von Adrichem, J. H.; Biro, M. C.; Kresbach, G. M.; Ehrat, M. *Rapid Commun. Mass Spectrom.* **1997**, *11*, 603–609.
(25) Williams, T. I.; Saggese, D. A.; Wilcox, R. J.; Martin, J. D.; Muddiman, D. C. *Rapid Commun. Mass Spectrom.* **2007**, *21*, 807–811.
(26) Borchardt, R. T. *Pharmaceutical Profiling in Drug Discovery for Lead Selection*; AAPS Press: Arlington, VA, 2004.
(27) Rodante, F.; Tocci, M. J.; Onofri, A. *Thermochim. Acta* **1985**, *88*, 347–353.
(28) Mcgarry, P. F.; Jockusch, S.; Fujiwara, Y.; Kaprinidis, N. A.; Turro, N. J. *J. Phys. Chem. A* **1997**, *101*, 764–767.
(29) Huo, Q.; Russell, K. C.; Leblanc, R. M. *Langmuir* **1998**, *14*, 2174–2186.
(30) Baluya, D. L.; Garrett, T. J.; Yost, R. A. *Anal. Chem.* **2007**, *79*, 6862–6867.
(31) Gosalia, D.; Diamond, S. L. *Methods Mol. Biol.* **2010**, *669*, 69–78.
(32) Tu, T.; Sauter, A. D., Jr.; Sauter, A. D., 3rd; Gross, M. L. *J. Am. Soc. Mass Spectrom.* **2008**, *19*, 1086–1090.
(33) Fournier, I.; Marinach, C.; Tabet, J. C.; Bolbach, G. *J. Am. Soc. Mass Spectrom.* **2003**, *14*, 893–899.
(34) Karas, M.; Gluckmann, M.; Schafer, J. *J. Mass Spectrom.* **2000**, *35*, 1–12.
(35) Wolski, W. E.; Lalowski, M.; Jungblut, P.; Reinert, K. *BMC Bioinf.* **2005**, *6*, 203.
(36) Humblet, V.; Misra, P.; Frangioni, J. V. *Contrast Media Mol. Imaging* **2006**, *1*, 196–211.
(37) Lee, P. J.; Chen, W.; Gebler, J. C. *Anal. Chem.* **2004**, *76*, 4888–4893.
(38) Wei, J.; Buriak, J. M.; Siuzdak, G. *Nature* **1999**, *399*, 243–246.
(39) Knochenmuss, R.; Zenobi, R. *Chem. Rev.* **2003**, *103*, 441–452.
(40) Kutt, A.; Leito, I.; Kaljurand, I.; Soovali, L.; Vlasov, V. M.; Yagupolskii, L. M.; Koppel, I. A. *J. Org. Chem.* **2006**, *71*, 2829–2838.